



Universiteit  
Leiden  
The Netherlands

## Mesenchymal stem cells in skeletal muscle regeneration

Garza-Rodea, A.S. de la

### Citation

Garza-Rodea, A. S. de la. (2011, September 28). *Mesenchymal stem cells in skeletal muscle regeneration*. Retrieved from <https://hdl.handle.net/1887/17877>

Version: Corrected Publisher's Version

License: [Licence agreement concerning inclusion of doctoral thesis in the Institutional Repository of the University of Leiden](#)

Downloaded from: <https://hdl.handle.net/1887/17877>

**Note:** To cite this publication please use the final published version (if applicable).

# Chapter 4

## **Pressure ulcers: description of a new model and the use of mesenchymal stem cells for repair**

AS de la Garza-Rodea, S Knaän-Shanzer, DW van Bekkum  
Accepted with a minor revision

## Abstract

### Background

Pressure ulcers (PU) still present a heavy burden on many patients and nursing institutions. Understanding the pathophysiology and development of new treatments is hampered by scarcity of suitable animal models.

### Objective

Evaluation of the translational value of an easily accessible mouse model.

### Methods

PU were induced by application of magnetic devices on the skin of mice. The extend of the lesions and healing time were quantified. Detailed histological analysis of the regeneration is presented.

### Results

Ulcers induced by this form of ischemia have many features in common with decubitus in humans. Unexpectedly, healing was not delayed in diabetic mice, but X-irradiation of the skin caused a substantial slowing of repair. Intradermal transplantation of mesenchymal stem cells (MSC) did not accelerate healing.

### Conclusion

The results emphasize the unique characteristics of PU as compared to surgical wounds. This experimental model is recommended for preclinical research on decubitus.

## Introduction

Pressure ulcers (PU) or decubitus continue to represent a heavy burden on many patients and nursing institutions. In spite of the availability of effective preventive measures, this complication is hard to avoid in certain categories of patients. The main predilection factors are old age, malnutrition, diabetes and paraplegia. Once an ulcer has developed, treatment is time and labour consuming and not always successful. The development of new therapeutic agents suffers from the lack of suitable animal models that allow rapid screening at low costs.

It is generally assumed that decubitus develops as a result of prolonged pressure on the skin and underlying tissues. This causes an interruption of the capillary blood flow and ischemia of the exposed tissue, leading to necrosis and ulceration.

The animal models thus far described in the literature employ a variety of devices to apply prolonged localized pressure on the skin, usually on surfaces overlying bone. These devices include a cuff applied to a leg or the tail of rats<sup>1</sup>, a walking cast on the hind leg of greyhounds<sup>2</sup>, electromechanical and air driven apparatus to deliver pressure to the skin above the trochanter major of rats<sup>3</sup>, pigs<sup>4-5</sup> and dogs<sup>6</sup>. All these procedures are cumbersome and need extended and repeated immobilization and anesthesia.

A major improvement was introduced by Pierce *et al.*<sup>7</sup>, who applied magnetic force on the full skin of rats by external magnets and a subcutaneously implanted iron plate. This allows ischemic exposure without anesthesia, but it requires initial surgery and can not be used in mice due to the weight of the iron plate (122 g). The latter problem was elegantly solved by using two opposing magnets, one of which was surgically positioned under the skin<sup>8</sup>. An even simpler technique was introduced by Stadler *et al.*<sup>9</sup> by clamping a dorsal skin fold between two opposing external magnets. Given adequate magnetic strength and exposure time two symmetrical ulcers are induced on the back of the animal. Except for shaving the dorsal area of hairy rodents, intervention is minimal and with the magnets in place the animals move, feed and drink normally. In these models ischemic damage is also induced in striated muscle due to the presence of the *panniculus carnosus muscle* (PCM) in the skin.

Surprisingly, this convenient and animal-friendly model has only been used so far by the inventors' group in Rochester NY for experimental laser therapy<sup>10-11</sup> and to study cytokines involved in ischemia-reperfusion (IR) cycles<sup>12</sup>. In these studies the mice are routinely exposed to three cycles of 12 hours ischemia and 12 hours reperfusion using 1000 G magnetic force which generates a pressure of 50 mmHg, the equivalent of 6.5 kPa.

Unaware of these data, we employed a similar technique to produce PU in the dorsal skin of mice. We used stronger magnets and a pressure of 75 kPa

(562.5 mmHg) that induces full thickness ulcers in a single ischemic session and we followed repair until epithelization was completed. As far as the descriptions allow, the lesions induced by the Rochester group are similar to the ones induced with our stronger magnets and shorter exposures. Both methods cause destruction of all skin layers in the compressed area. The abrupt development of the injury in these models is much the same as with clinical PU. So far the models have been explored in a limited way. In the publication of Stadler *et al.*<sup>9</sup> only one pressure exposure regimen is described, and Reid *et al.*<sup>8</sup> studied only the acute phase of the injury for up to 10 days.

In the present study, the effect of various ischemic times on the skin of hairless as well as hairy mice were studied. The latter included NOD/SCID mice in preparation for studies on the effect of treatment with human mesenchymal stem cells (MSC).

The PU produced with external magnets healed within 12-20 days depending on the duration of ischemia. In this respect, the model may not be realistic as the decubitus problem in human patients is its slow healing. The delayed wound repair in patients is attributed to poor general condition, inadequate local blood circulation and abnormal metabolism or vascularisation as in diabetes. Whenever a PU develops in a healthy person, recovery is as fast as of any other wound and the same applies to normal laboratory mice. As this probably represents the maximal repair rate, it seemed unlikely that it can be improved by treatment. Therefore, modification of the mouse model to achieve slower healing was attempted for research into new ways of treatment.

The healing of surgical skin wounds has been reported to be delayed in diabetic mice<sup>13-16</sup> but the underlying mechanisms are not well understood. Local irradiation is also known to interfere with the healing of surgical wounds, clinical<sup>17</sup> as well as experimental<sup>18</sup>. It is not known if pressure wounds respond similarly to diabetes and irradiation as surgical skin wounds. Accordingly, we have used the decubitus model in the mouse to investigate these issues. We found that the diabetic condition does not affect the healing but that irradiation delays repair of the epidermis and prevents complete regeneration of dermis and hypodermis until at least 3 months after wounding.

## Materials and Methods

### Isolation and culture of MSC

All experiments were performed with bone marrow (BM) cells of a 38-year-old female collected with informed consent during orthopaedic surgery according to the guidelines of the Leiden University Medical Center (LUMC). MSC were isolated from the BM sample as described previously<sup>19</sup>. The cells were cultured in Dulbecco's modified Eagle medium, 100 U/ml penicillin, 100 µg/ml

streptomycin and 10% fetal bovine serum (all from Invitrogen) and incubated at 37°C in humidified air with 10% CO<sub>2</sub>. At passage number 2, aliquots of 2×10<sup>5</sup> cells were cryopreserved. For the expansion of the MSC in plastic 25-cm<sup>2</sup> cell culture flasks (CELLSTAR; Greiner Bio-One, Frickenhausen, Germany) the same culture conditions were used except for the addition to the growth medium of basic fibroblast growth factor (Sigma-Aldrich, St. Louis, MO) to a final concentration of 0.5 ng/ μl. The characterization of the cultured BM-derived MSC was by immunophenotyping and *in vitro* differentiation assays<sup>19,20</sup>.

### Lentiviral transduction of MSC

BM-derived MSC were transduced with the vesicular stomatitis virus G protein-pseudotyped self-inactivating human immunodeficiency virus type 1 vector LV.C-EF1a.bGal<sup>21</sup> to generate LacZ-MSC. Twenty-four hours after seeding at a concentration of 4×10<sup>4</sup> cells/cm<sup>2</sup>, MSC were incubated for 4 hours at 37°C with vector particles at a multiple of infection of 2 Hela cell-transducing units per cell in growth medium containing 8 μg/ml hexadimethrine bromide (Sigma-Aldrich)<sup>21</sup>. Transduction efficiency was determined 14 days later by staining the cells with X-gal solution containing 2 mM 5-bromo-4-chloro-3-indolyl-β-D-galactosidase (X-gal; Sigma-Aldrich)<sup>22</sup>. More than 90% of the cells were β-gal<sup>+</sup> at this time point as well as after multiple *ex vivo* cell doublings. After transduction, the cells were passaged twice and cryopreserved until further use. Before the start of an *in vivo* experiment, aliquots of the LacZ-MSC were thawed and expanded for up to 4 additional passages to obtain the required numbers of cells.

### Animals

Male and female mice aged 5 to 20 weeks were used. Hairless SKH1-*hr* mice were purchased from Charles River Laboratories International, Inc. (Wilmington, MA, USA) and the MF1-*hr* mice from Harlan Laboratories (Indianapolis, IN, USA).

Inbred *NOD-LtSz-scid/scid/J* (NOD/SCID) mice were from the animal breeding facilities of LUMC. This colony was established with mice originally purchased from Jackson Laboratories (Bar Harbor, ME, USA). The mice were kept and housed as previously described<sup>23</sup>. All experimental procedures were approved by the local Experimental Animal Ethics Committee.

### Induction of PU

Pressure is applied to the upper part of the dorsal skin of unanesthetized mice by applying two opposing magnetic disks on the central skin fold for a certain

period of time (4, 8, 12, 14 or 20 hours). The magnets are held in place by the magnetic force which is equivalent to a pressure of approximately 75 kPa (562.5 mmHg) on the skin fold (Figure 4.1A). The reperfusion was clearly demonstrated when injected intravenously the vital dye Patent Blue V (Guerbet, France) in a mouse a few minutes before removal of magnetic disk after 7 hours of clamping (Figure 4.1B). The pressure was measured by estimating the weight required to pull the disks apart when placed on both sides of a 1 mm thick piece of cardboard simulating the skin fold of the mouse. The disks consist of a polyvinyl chloride (PVC) casing containing a 0.47 T (4700 G) NdFe35 magnet. The surface of the disks is circular with a diameter of 12 mm and the weight is 2.5 g. In the case of hairy mice, the dorsal skin was shaved with electric clippers prior to the application of the disks. Mice are placed in individual cages when carrying the disks to prevent magnetic interaction. After the disks have been removed, the mice are housed together with up to 4 per cage and inspected daily. As soon as the injured skin has changed to a homogenous brownish patch (3-4 days), the surface of the lesions is measured regularly using a Vernier caliper with the mice under light inhalation anesthesia with isoflurane (Piramal Healthcare, London, England). The largest (a) and the smallest (b) diameter of each lesion are recorded and the ulcer surface is calculated using the formula  $\pi ab/2$ .

In few mice a single confluent lesion developed centrally on the skin of the back due to displacement of the magnets. These mice were excluded from evaluation.

### Induction of diabetes

Two different lots of streptozotocin (STZ, Sigma-Aldrich) were used which contained 88.0% and 88.4% of the alpha anomer as specified by the manufacturer. The dry powder was dissolved in 0.1 M of sodium citrate buffer, pH 4.5. Control and experimental groups were injected intraperitoneally once with 300  $\mu$ l of sodium citrate buffer only or stabilized STZ solution at dose 150 or 160 mg/kg respectively<sup>24</sup>. The stabilized solution was injected 2-3 hours after dissolution. For storage stabilized STZ solutions were kept in the dark at 4°C. Body weight and non-fasting blood glucose levels were monitored weekly. Blood samples were obtained from tail cuts. Glucose was determined with a glucometer (Accu-Check Sensor, Roche, Germany). The upper limit of this assay is 33.3 mmol/l. Blood samples reaching this limit were recorded as such for the calculations. Mice with glucose levels over 11 mmol/l (200 mg/dl), were classified as diabetic<sup>14</sup>.

Magnetic disks were applied in diabetic mice between 15 to 35 days after hyperglycemia was first detected.

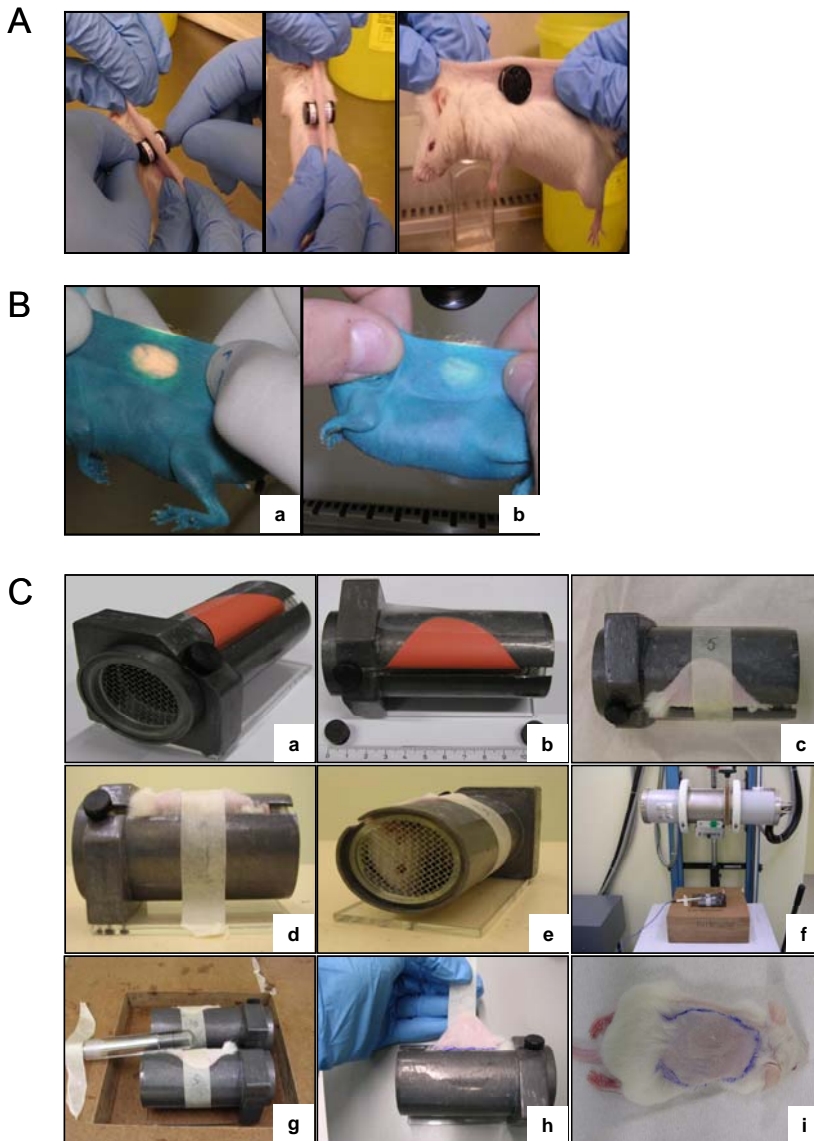


Figure 4.1 **PU model and device for skin irradiation.** A: position of magnetic disks placed on dorsal skin fold of hairless mouse. B: vital dye Patent Blue V was administered intravenously a few minutes before removal of the magnetic disks after 8 hours of clamping. (a) 30 seconds and (b) 15 minutes of reperfusion. C: lead cylinder of 2 mm wall thickness used to irradiate skin. The dorsal skin fold of a mouse is pulled out along one side of the cylinder and fixed upwards with tape as demonstrated with surrogate skin in (a) and (b); (c) and (d) position of shaved skin flap; (e) position of NOD/SCID mouse; (f) irradiation set up; (g) dosimeter in place; (h) release of skin flap after irradiation and (i) marked irradiated area.



## Irradiation of the dorsal skin of mice

Male and female NOD/SCID mice were anesthetized by i.p. injection of a mixture of Ketamine hydrochloride (100 mg/kg; Nimatek, Eurovet Animal Health, Bladel, the Netherlands) and Xylazine hydrochloride (10 mg/kg; Rompun, Bayer AG, Leverkusen, Germany). As presented in Figure 4.1C the back of anesthetized mice was shaved and the mice were placed inside a lead cylinder of 2 mm wall thickness with a 6 cm wide slit along one side. For irradiation exposure the dorsal skin fold of the mice is pulled out through the slit and fixed upwards on the cylinder with tape. The area of exposed skin was marked. Two cylinders were positioned inside the radiation field 30 cm below the X-ray tube of an orthovolt X-ray generator (Gullmay Medical Lt, UK) that was operated at 120 kV, 8 mA using a 0.5 mm Al filter. The half value layer (HVL) of the radiation was 2.5 mm Al. Dose rate on the exposed skin fold was 1.3 Gy/min. The dose to the skin was 8 Gy. Total body exposure was 0.3% of the dose on the skin fold. Dose measurement was performed with a Unidos E Universal Dosimeter (PTW, Freiburg Germany) using chamber 01. Magnets were applied between 1 and 2 hours after irradiation within the irradiated area.

## Cell transplantation procedure

Male and female NOD/SCID mice aged 8 to 12 weeks were used to evaluate the effect of BM derived MSC implantation on decubitus.

Decubitus was induced by 12 hours of pressure. Three hours after magnet release  $5 \times 10^5$  LacZ-MSC suspended in 40  $\mu$ l of phosphate saline buffer (PBS) were injected in two portions into opposing edges of the ulcer (Figure 4.8). Irradiation, if included in the experimental setting, was delivered as previously described before the induction of ischemia.

## Histology

Ulcerated areas were dissected with a wide margin of normal skin at various intervals after reperfusion. The samples were stretched ,epidermis upwards, on filter paper, cut in 2 equal halves and fixed overnight in 4% phosphate-buffered formaldehyde (PFA, Mallinckrodt Baker, Phillipsburg, NJ) at 4°C prior to embedding in paraffin. Six- $\mu$ m-thick sections perpendicular to the skin surface were stained with hematoxylin, phloxin and saffron (HPS) using a standard procedure.

For cell transplantation experiments ulcers/scars were excised at 10, 30 or 60 days, placed in filter paper, divided into two equal parts and fixed in 4% PFA for 1 hour at room temperature. Fixed tissues were stained with X-gal and embedded in paraffin as reported before<sup>21</sup>. Six- $\mu$ m-thick serial transversal cross-sections were made and co-stained with HPS.

Analysis and capture of images were performed with a digital camera (ColorView Illu; Olympus, Zoeterwoude, the Netherlands) mounted on an Olympus BH-2 microscope and processed with the aid of Olympus Cell<sup>F</sup> software.

## Immunohistochemistry

Satellite cells in the PCM of decubitus sections were stained with the Pax7 antibody. Briefly, sections were deparaffinized and rehydrated by xylene (twice for 10 minutes each) and subsequently with in various ethanol dilutions (100%, 96%, 70% and 50%, 5 minutes each). Tissues were then washed three times with PBS for 5 minutes each. For antigen retrieval sections were boiled in sodium citrate buffer pH 7.4 (10 mM; 10 minutes). Sections were cooled to room temperature prior to incubation with 0.3% hydrogen peroxide at room temperature for 10 minutes. After three more PBS washes a 1-hour incubation with 10% normal goat serum (Dako, the Netherlands, Heverlee, Belgium) in a moist chamber was performed to block non-specific bindings. Next, the monoclonal chicken antibody specific to Pax7 (Developmental Studies Hybridoma Bank, Iowa, City, IA) was added to each tissue section and incubated overnight at 4°C in a moist chamber. Next day the sections were washed in PBS and incubated for 30 minutes with polyclonal horseradish peroxidase-conjugated goat anti mouse IgG antibody in a moist chamber. Immunoreactivity was visualized with 3, 3'-diaminobenzidine (DAB, Sigma-Aldrich). Finally, sections were counterstained with hematoxylin and saffron and mounted in Pertex mounting medium (Histolab, Gothenburg, Sweden). Analysis and capture of images were performed as described above.

## Statistical analysis

Wound surface data were expressed as mean  $\pm$  SEM.

## Results

### Effect of ischemic time on PU size and healing course

Immediately after removal of the magnets, the compressed area appears pale and bloodless. Intravenous injection of a vital dye Patent Blue V confirms that the circulation has been disrupted (Figure 4.1B). Perfusion of the area is re-established within about 30 minutes. These observations demonstrate that the induction of PU by this method is due to IR, similar to the mechanism assumed to prevail in the causation of clinical bed sores.

During the first 48 hours of reperfusion the compressed areas of skin on the back of the mouse, one at each side of the dorsal midline, take on a yellowish color with erythematous patches. By day 3 or 4 after reperfusion, the lesions turn dark brown and a crust develops. On some an exudate appears during these early stages. From then on the lesions begin to shrink until the last of the crust has disappeared. Complete re-epithelization is reached in 10 to 20 days depending on the duration of the ischemic period (Figure 4.2 and 4.3).

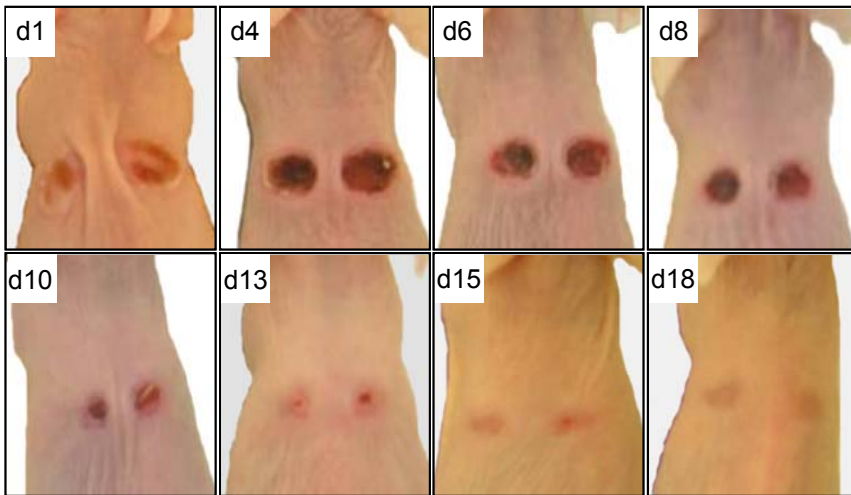


Figure 4.2 Macroscopic appearance of PU (12 hours of ischemia) in a single SKH1 mouse at different time points after reperfusion.

The rate of repair is graphically depicted in Figure 4.3 for hairy and hairless mice respectively following ischemic exposure times from 4 to 20 hours. There is a trend for the ulcers to be larger and to heal slower with increasing ischemic time. In addition, the wound surfaces in hairy and hairless mice regress at similar rates until  $\pm 5 \text{ mm}^2$ . The final part of healing, being basically the disappearance of all scab, is prolonged in hairy mice (Figure 4.3B). Following 20 hours of pressure, most hairless mice developed a single large ulcer covering the two pressed skin surfaces as well as varying parts of the skin in between. As this prevented accurate measurements of the lesions we chose to use a standard period of 12 hours pressure in subsequent experiments.

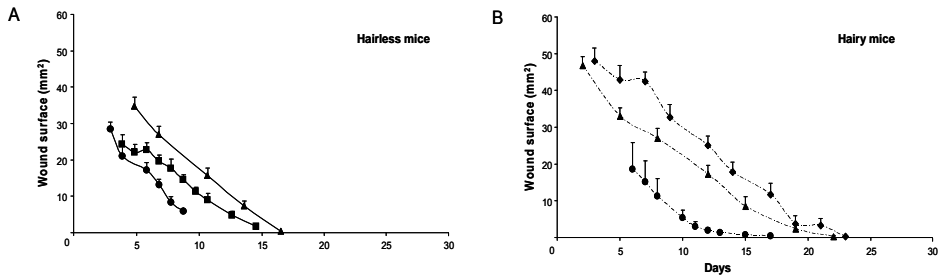


Figure 4.3 **Rate of healing of ulcers in three mouse strains following different periods of pressure.** Average of calculated surface (see Material and Methods) of ulcers is plotted. A: hairless mice after 4 hours (●; SKH1; N=26), 8 hours (■; MF1; N=24) and 12 hours (▲; SkH1; N=30) of ischemia. B: hairy mice (NOD/SCID) after 7 hours (●; N=6), 12 hours (▲; N=13) and 20 hours (◆; N=14) of ischemia. Vertical bars: SEM.

## Histology of PU

Histological analysis of the injured skin was performed systematically in SKH1 mice at various intervals after an ischemic period of 12 hours (Figure 4.4). The normal skin of SKH1 mice contains typical structures such as epidermal utriculi - assumedly remnants of the hair shaft - and numerous dermal cysts and granulomas.

At 8 hours after reperfusion, the compressed area can already be clearly distinguished by the presence of epidermolysis and blister formation with beginning necrosis of the underlying tissues including the PCM. There is a clear demarcation between the compressed skin, and the undamaged surrounding tissues. Slight infiltration of granulocytes and monocytes is observed at this time in the border areas of the skin lesions. In all aspects these lesions resemble severe PU in humans, except that bone is obviously not involved.

At 24 hours, the basal layer of the epidermis, dermis and the fat cells of the subcutis (hypodermis) are necrotic. The subcutaneous tissue shows hemorrhages and edema and is infiltrated by inflammatory cells. The PCM is heavily infiltrated and in some places the muscle fibers are necrotic; in other parts, nuclei and striations are still apparent.

At 48 hours a crust has started to form over the lesion. All tissue layers in the central area are now necrotic and there is massive infiltration of the PCM by inflammatory cells.

At 4 days underneath the crust regeneration is starting from the undamaged border tissues. The epidermis in the periphery of the ulcer shows a thick layer of cells indicative of active proliferation. In the muscle layer the myoregeneration has started as well, myoblast and small myofibers with central nuclei are located at the edges of the wound.

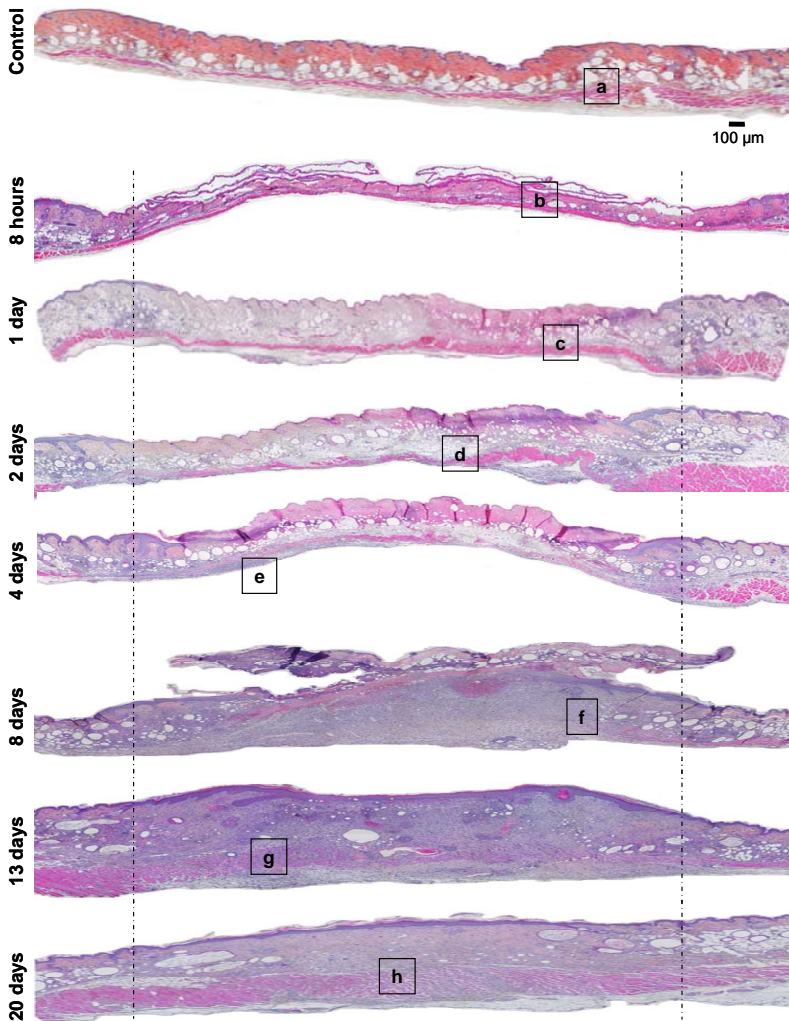


Figure 4.4 **Microscopic appearance of pressure ulcers**. in SKH1 mice at different time points after reperfusion. Ulcers were induced by 12 hours of ischemia.. A: HPS stain. Broken lines mark margins of the lesion. B: pictures of PCM taken from marked locations of A. (a) undamaged PCM; (b) destroyed dermis and necrotic PCM; arrows in (c) and (d) indicate cell infiltrates; arrow heads in (e) indicate nascent myofibers coming from the edges of the lesion; (f) and (g) newly formed myofibers with central nuclei and heterogeneous sizes; (h) remodeling of central part of PCM in progress. Magnifications A: 100 $\times$ ; B: 200 $\times$ .

In the following days the epidermis continues to grow towards the centre of the lesion, pushing out the crust. In some cases a second, smaller, crust developed between 6 to 10 days. The necrotic PCM moves to the surface with

the crust around day 10 and a regenerating muscle layer is proceeding from the edges of the wound.

Around day 13 the epidermis has closed and a scar has formed. However, remodeling as well as regeneration of the underlying tissues is continuing. The epidermis is still thicker than normal. In the dermis many mesenchymal cells are present as well as granulation tissue, and formation of appendages continues. At this time, the regenerating PCM has proceeded to the centre of the ulcer

At day 20 the epidermis has reached almost normal thickness; in the dermis the cellular infiltrate has decreased and new collagen is clearly apparent. Some of the skin appendages have developed. The PCM still shows active regeneration with a remarkably increased number of myofibers (thick layer) that are still not fully arranged. The ulcers analyzed over time from hairy mice (i.e. NOD/SCID) revealed a similar pattern of repair.

### Healing rate of PU in diabetic mice

Experimental diabetes was successfully induced with streptozotocin (STZ). Most of the hairless (SKH1) or hairy (NOD/SCID) mice presented with hyperglycemia (>200mg/dL) approximately 2 weeks after injection of STZ. Increased blood glucose levels did not affect body weight when compared to control mice (data not shown).

Contrary to expectations, diabetic mice showed a normal rate of healing of pressure ulcers (Figure 4.5). We investigated both hairless and hairy mice, different pressure exposures (7 to 20 hours) and mice that suffered from hyperglycemia for different periods of time (15 to 35 days). Under all conditions tested no differences were seen with the controls (Figure 4.5). Microscopically, the recovery in epidermis, dermis and PCM in the diabetic mice was also similar to that in control mice (data not shown).

### X-irradiation delays wound healing

The effect of prior skin irradiation was investigated in NOD/SCID mice as these permit the grafting of human mesenchymal stem cells (MSC), which was part of this study. For surgical wound healing in normal mice as measured by breaking strength of the wound at 14 days the dose response curve shows a maximal decrease after a dose of 20-25 Gy<sup>18</sup>. The tissues of NOD/SCID mice are known to be roughly 3 times as sensitive to ionizing radiation as those of normal mice<sup>25</sup> due to a defect in double strand break repair of DNA. Accordingly, an irradiation dose of 8 Gy was chosen, which resulted in roughly a doubling of the healing time (Figure 4.6). Mild erythema and dry desquamation of epidermis of the irradiated skin was noted in the majority of mice beginning at day 12 and

resolving around day 30 (Figure 4.6A) which is in agreement with the dose response curves for acute dermatitis published by Budach *et al.*<sup>25</sup>.

There is a distinct delay of PU healing in pre-irradiated mice as shown in Figure 4.6B which contains pooled data of two similar experiments. Histological analysis confirms that irradiation slows down the regeneration of the epidermis (Figure 4.6C). There is a greatly delayed repair of dermis and even at 90 days post injury there is no formation of appendages although collagen fibers are normally arranged. No repair of PCM is apparent (Figure 4.6C). Immunohistochemical analysis with antibodies specific for satellite cells (Pax7) revealed a greatly reduced number in the irradiated skin at 8 days as compared to non-irradiated skin (control, Figure 4.6D). It suggests that irradiation with 8 Gy depletes most of the satellite cells of the PCM. In non-irradiated lesions the number of satellite cells decreases over time and muscle regeneration is not complete even at 90 days post injury as evidenced by heterogeneous sizes of the myofibers. In the irradiated skin no signs at all of muscle regeneration (nuclei centralized) were observed; rather the PCM remains composed of dispersed myofibers with peripheral nuclei.

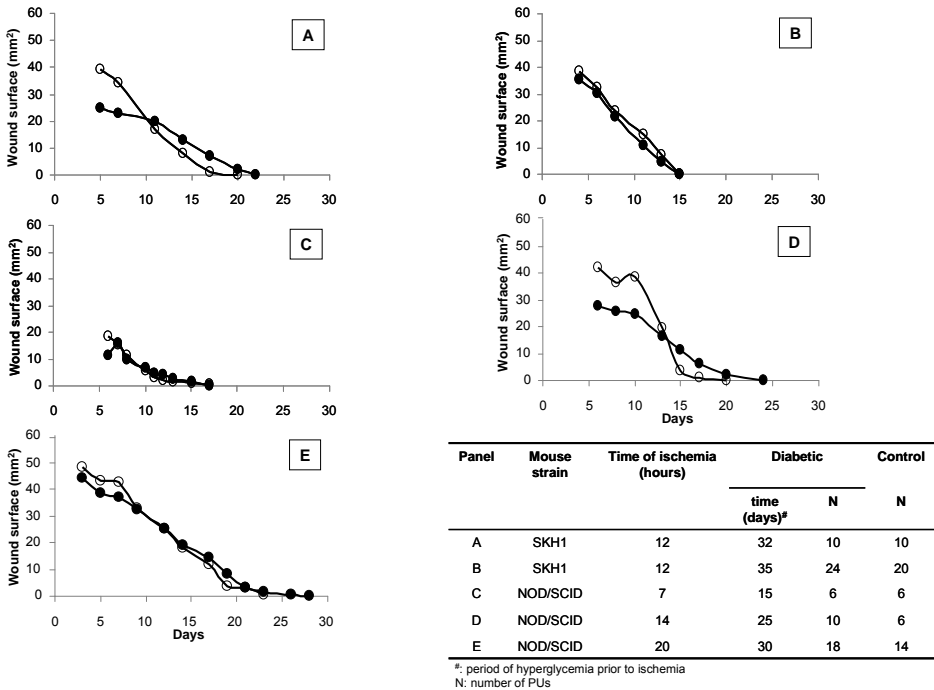
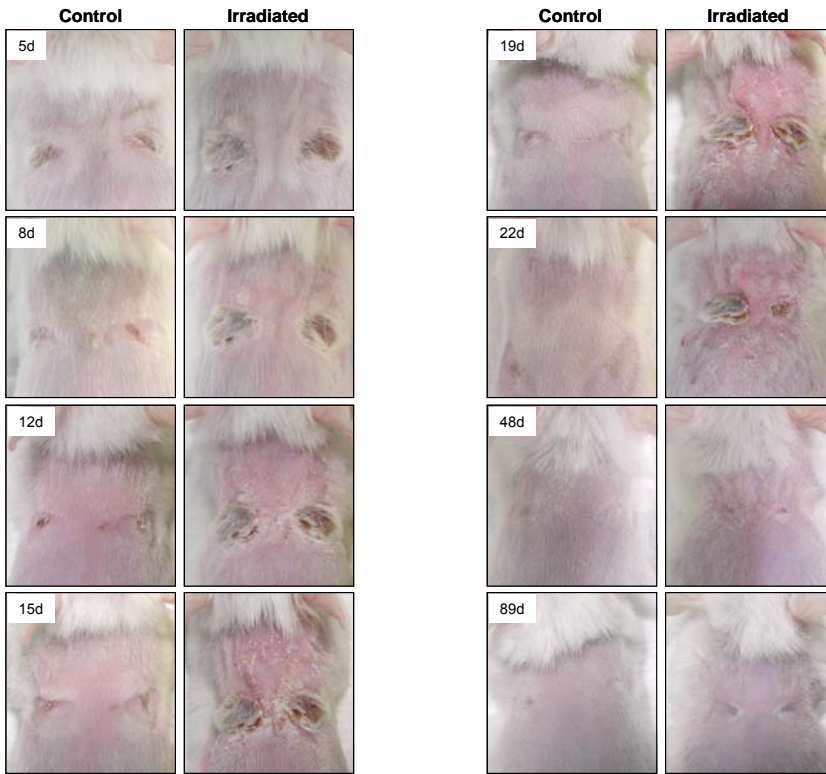
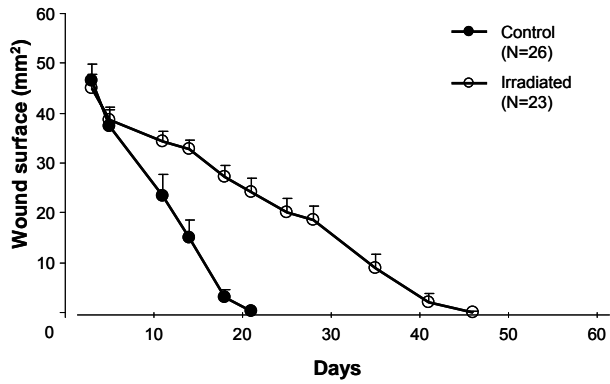


Figure 4.5 **Rate of healing of PU in diabetic and control mice.** Averages of calculated ulcer surface are plotted. Hairless (A and B) and hairy mice (C,D,E). Diabetics (closed circles); controls (open circles). Ischemic time and number of animals are listed in the inserted table.

A



B





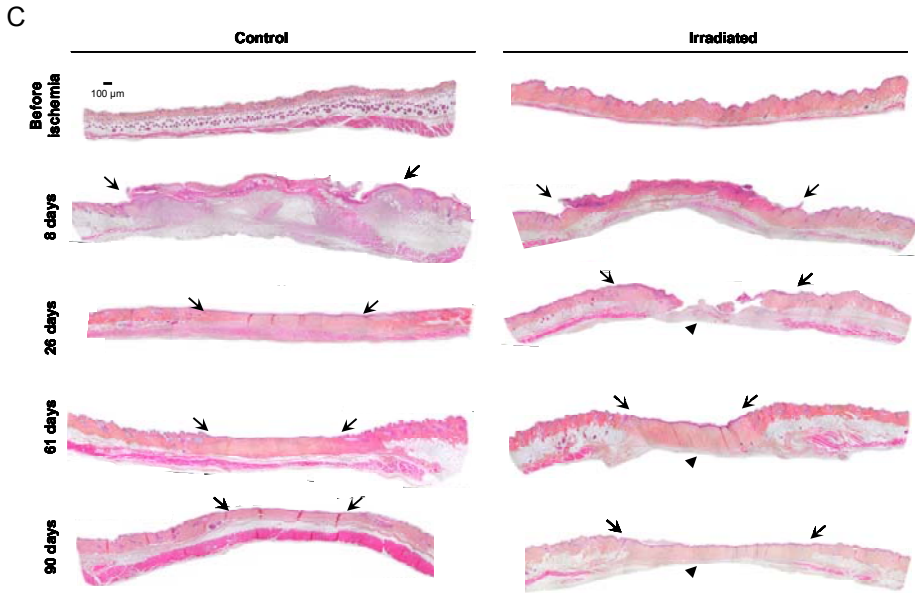


Figure 4.6 **Effect of pre-irradiation of the skin on decubitus.** Lesions were induced by 12 hours of ischemia. A: macroscopic appearance of irradiated and control lesions in NOD/SCID mice over time. Note mild dry dermatitis in irradiated skin from day 12 to 22. B: rate of healing of pre-irradiated (open circles) and control PU (closed circles). C: microscopical appearance of ulcers stained with HPS; arrows mark margins of the lesion; arrow heads point at areas of PCM without regeneration. Magnification: 100 $\times$ . D: photomicrographs of PCM in pre-irradiated and control decubitus. Sections stained with antibody specific for satellite cells (Pax7). Nuclei counterstained with hematoxylin. Arrows indicate satellite cells positive to the antibody. Magnification: 400 $\times$ .

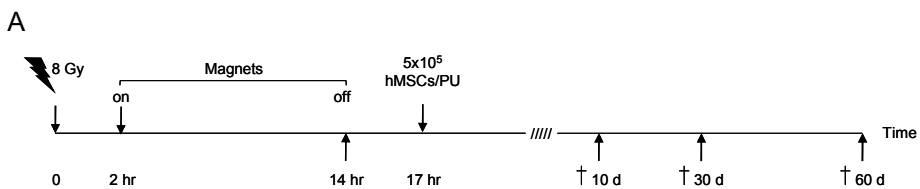
### Transplantation of MSC in decubitus

Various modes of injection were compared in NOD/SCID mice to find the best delivery of the MSC into the lesion. Eventually we chose to inject  $5 \times 10^5$  LacZ-MSC intradermally (see Materials and Methods) into control and pre-irradiated normal skin. The cells were found to be reproducibly deposited in the dermis in tight clusters with no signs of migration or spreading from the site of injection. The size of the clusters decreased over time. Away of the cluster no  $\beta$ -galactosidase-positive ( $\beta$ -gal<sup>+</sup>) cells were present (Figure 4.7B).

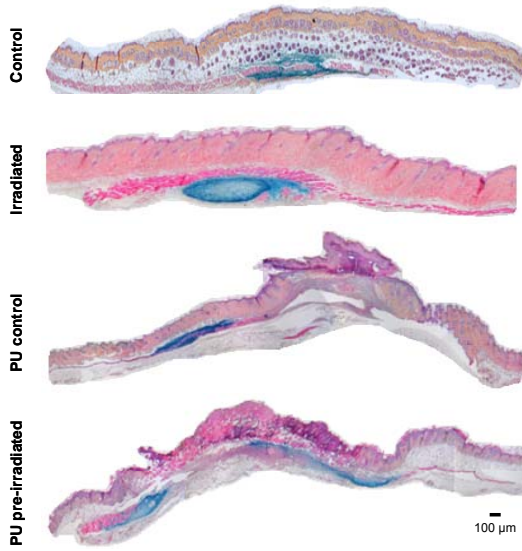
Treatment with MSC did not enhance the healing of the pre-irradiated PU in any way. The rate of repair of the pre-irradiated PU was similar with or without addition of LacZ-MSC (Figure 4.8). The fate of the cells was tracked microscopically in control PU and pre-irradiated PU and was found to be similar at 10 and 30 days after injection (Table 4.1).

At 10 days LacZ-MSC were distributed adjacent to the edges of the lesion in dermis and PCM. At that time all layers of skin (i.e. epidermis, dermis and PCM) showed active regeneration from the edges inwards (Figure 4.7B). In the pre-irradiated PU the re-epithelization was less advanced. There were cell infiltrates at the demarcation of the damage area. *LacZ* expression was observed in a few cells with the morphology of fibroblasts, adipocytes, endothelial cells and myoblasts (Figure 4.7C). Occasionally,  $\beta$ -gal<sup>+</sup> cells were seen in nerve tissue.

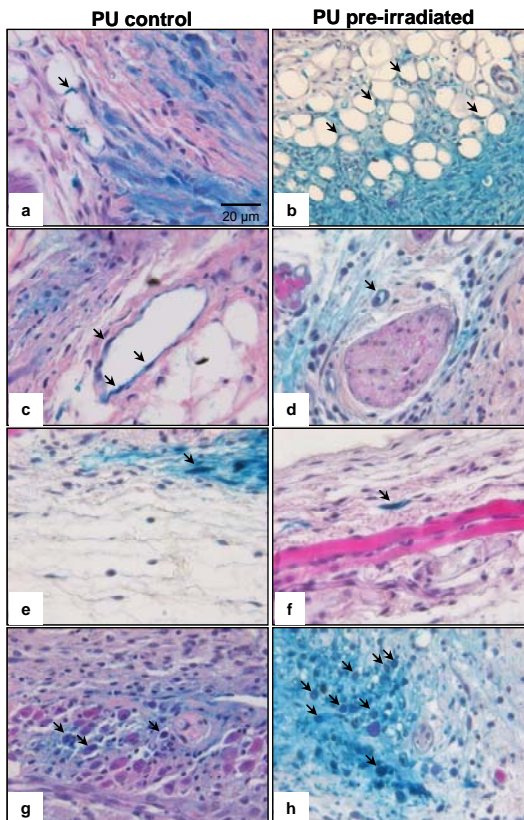
At 30 days regeneration of epidermis was complete in both groups (Figure 4.7D). Dermis and PCM presented similar features as non-treated PU and non-treated pre-irradiated PU as described earlier. At this time point LacZ-MSC had not migrated further into the surroundings and transdifferentiated cells were no longer seen. However, a few,  $\beta$ -gal<sup>+</sup> myofibers were observed in the PCM at the edge of the original lesion. Two types of *LacZ*-expressing fibers could be distinguished: short fibers that stained entirely blue and mosaic fibers containing blue segments (Figure 4.7E) as occurred in the cardiotoxin-injured *tibialis anterior* muscles similarly treated with LacZ-MSC<sup>21</sup>. Further at this time, the PCM of the control PU had been fully restored but there was no repair of the pre-irradiated PCM (Figure 4.7D). Therefore the latter were also examined at 60 days and still there was no regeneration of the muscle (Figure 4.7F) as observed before in non-treated pre-irradiated PU (see section Irradiation delays wound healing). At this time point epidermis and dermis were restored to their normal thickness. The collagen fibers of dermis were normally arranged but the appendages were still absent. At the edges of the scar few single *LacZ* expressing MSC are still present but no transdifferentiation of cells was apparent. Some blue  $\beta$ -gal<sup>+</sup> myofibers were detected in PCM (Figure 4.7F).



B



C



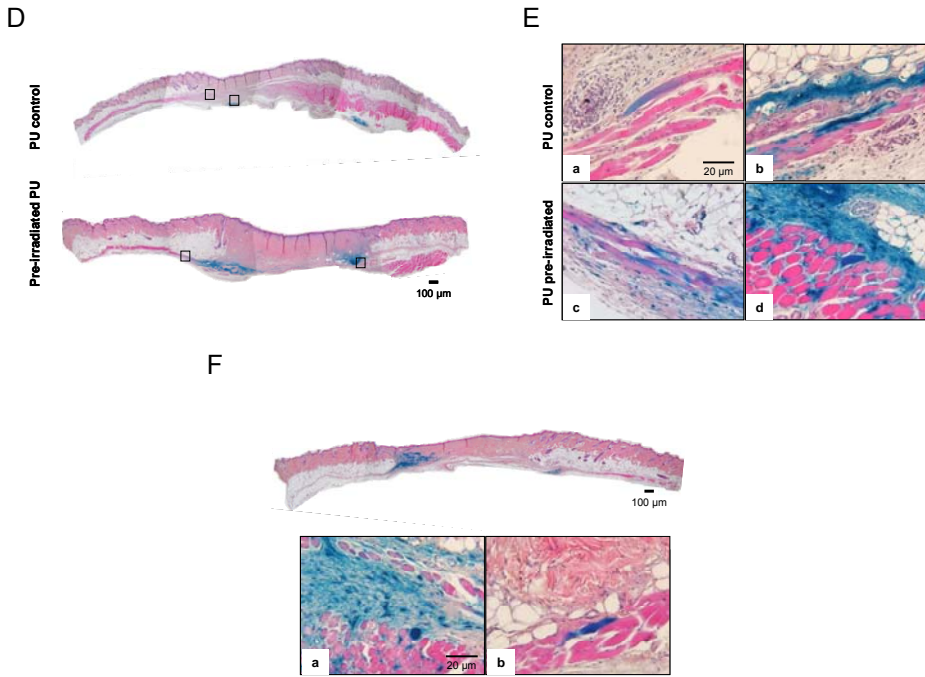


Figure 4.7 **Effects of intradermally injected MSC on decubitus.** A: time line of experiments. B: skin sections collected 10 days after LacZ-MSC injection. C: photomicrographs of subcutis from control PU and pre-irradiated PU 10 days post cell transplantation. (a and c) arrows indicate  $\beta$ -gal+ adipocyte-like cells; (c and d) arrows indicate  $\beta$ gal+ endothelial-like cells; (e and f) arrows indicate  $\beta$ -gal+ fibroblasts; (g and h) PCM in regeneration characterized by presence of myoblast-like cells and myofibers with central nuclei, some of them are  $\beta$ -gal+ (arrows). D: microphotographs of control and pre-irradiated PUs at 30 days post MSC transplantation. E: Higher magnification of D (a and c) mosaic myofibers, (b) completely blue myofiber, (d) transversal section of PCM with a blue myofiber. F: photomicrographs of pre-irradiated PU collected at 60 days after MSC injection. MSC are still located at the site of injection. (a) the majority of the MSC are present as single cells; (a) and (b) blue myofibers. All tissue sections were stained with Xgal and counterstained with HPS. Magnifications: 100 $\times$  B,D and F; 400 $\times$  C,E and Fa and Fb.

Table 4.1 Histological findings in skin following injection of LacZ-MSCs.

Skin condition	Days post cell injection	Control (non-irradiated)	(Pre-) irradiation
Normal	10	LacZ-MSCs clustered No transdifferentiated mononuclear donor cells	LacZ-MSC clustered No transdifferentiated mononuclear donor cells
PUs	10	LacZ-MSCs spread & clustered Transdifferentiated mononuclear donor cells including few $\beta$ -gal <sup>+</sup> myoblast-like cells	LacZ-MSC spread and clustered Transdifferentiated mononuclear donor cells including few $\beta$ -gal <sup>+</sup> myoblast-like cells
	30	Decreased number of LacZ-MSCs No transdifferentiated mononuclear cells PCM fully regenerated Some $\beta$ -gal <sup>+</sup> myofibers*	Decreased number of LacZ-MSCs No transdifferentiated mononuclear cells No regeneration of PCM Some $\beta$ -gal <sup>+</sup> myofibers*
	60	ND	LacZ-MSCs still present No regeneration of PCM Some $\beta$ gal <sup>+</sup> myofibers*

PCM, panniculus carnosus muscle; ND, not done. \*only near the undamaged PCM

## Discussion

PU are a widespread and often underestimated health problem. They develop during periods of immobilization at sites where ischemia of the skin occurs as a result of compression between the body and an unyielding resistant surface. In severe cases, the underlying muscle and bone are also damaged. The National Pressure Ulcer Advisory Panel defines PU as “an area of unrelieved pressure over susceptible areas, such as bony prominences, resulting in ischemia, cell death and tissue necrosis”<sup>26</sup>. Even with the best possible medical and nursing care, PU may be hard to prevent in vulnerable people. Clinical research into pathogenesis and treatment is difficult because of the heterogeneity of the disease and limited possibilities for interventions.

Animal models are much needed to further understanding of the etiology and pathophysiology of PU, as well as to facilitate the development of new therapeutics. The majority of experimental PU require complicated pressure devices and laborious exposures and cannot easily be adapted to small laboratory rodents. Recently, several magnetic devices were introduced that simplify the induction of PU in small rodents<sup>7-9</sup>. We employed a modification of the procedure described by Stadler. Whereas Stadler and coworkers<sup>9</sup> as well as Saito and coworkers<sup>12</sup> used 3 successive cycles of 12 hours of ischemia and 12 hours of reperfusion, we induced lesions of roughly similar severity by a

single ischemic exposure of 12 to 14 hours. This may be due to the fact that we used much stronger magnets (0.47 versus 0.1 T). Accordingly, the pressure delivered to the skin fold is much higher in our case: 562.5 mmHg versus 50 mmHg. Possibly, in the studies with the weaker magnets, the lower pressure is compensated for by using repeated cycles of IR. Studies in rats<sup>7</sup> mice<sup>27</sup> and pigs<sup>4</sup> show cyclic exposures to be more damaging than a single session of the same total ischemic duration. On the other hand, our results are in close agreement with those of Park<sup>28</sup> who applied the same cyclic exposures as Stadler<sup>9</sup> and much stronger magnets (0.385 T). Unfortunately, in the study of Park the pressure on the skin is not reported. Because of these uncertainties it cannot be decided whether single sessions or repeated cycles of IR are the more relevant in translational terms. From clinical experience both modes of exposure produce decubitus.

As regards etiology, our model seems to be realistic enough in view of the observation that surgical procedures lasting longer than four hours and involving immobilization of the patients triple the risk of decubitus<sup>29</sup>. The advantages of our single session procedure are obvious: less labour intensive and less time consuming.

We have produced similar ulcers in rats using the same magnets in a slightly wider encasement (diameter 15 mm) after 16 hours of ischemia (data not shown), indicating that our procedure may be equally useful in other small rodents.

In the present extended histological analysis we show that the regeneration of the different skin components takes different times, epidermis to be the first to attain full recovery between 10 to 20 days, followed by dermis and PCM around 30 days and finally by the skin appendages that start developing between that time as well 30 days.

Surprisingly, the diabetic condition did not delay the healing of the PU. This finding was unexpected considering the many reports of delayed healing of excisional skin wounds in STZ induced diabetic mice<sup>13-14,16,30</sup> and rats<sup>15</sup>. Our negative results suggest differences in repair mechanisms between decubitus and surgical skin wounds. As pointed out by Trousdale<sup>31</sup> diabetic foot ulcers are associated with peripheral vascular disease, a macrovascular complication. Perhaps the increased tendency of diabetic patients to develop PU is due to impaired circulation in the lower limbs. Diabetic mice do not display this macrovascular disease, but instead exhibit decreased microvascularisation<sup>16</sup>. If the repair of excisional wounds were more dependent on microvascular circulation and that of PU more on macrovascular blood supply to the area, our diabetes dilemma would be solved.

On the other hand, pre-irradiation of the skin resulted in a clear cut delay of the repair of PU (Figure 4.6B) as is the case with surgical skin wounds<sup>17</sup>. This points to a common feature in the repair of the two forms of injury. The first that

comes to mind is the cellular repopulation that is dependent on the supply of stem cells from the surrounding intact skin and their subsequent proliferation. Irradiation affects all proliferative cell systems and hence inhibits regeneration of all tissues. We show that a dose of 8 Gy to the skin of NOD/SCID mice that is equivalent to about 20 Gy in normal mice, delays re-epithelization for almost 20 days. At 90 days post injury, regeneration of the appendages is not yet complete and the PCM shows no repair at all, due to the inactivation of the satellite cells by high dose ionizing radiation<sup>32-35</sup>.

The pre-irradiated PU is therefore very well suited for investigating the contribution of exogenous MSC to the regeneration of striated muscle, in this case the PCM, as participation of resident precursor cells is virtually excluded. For this purpose the MSC were injected shortly after reperfusion intradermally into the edge of the compressed area at two opposing sites. This treatment did not modify the size of the ensuing ulcers nor the course of healing (Figure 4.8). This lack of effect is somewhat surprising in view of several reports of acceleration of the closure of excisional skin wounds by treatment with MSC in mice<sup>36-38</sup> and rats<sup>39</sup>. In these studies cells were also administered intradermally and the numbers of cells administered were of the same order of magnitude, the main differences with our experiments being that the MSC were of syngeneic origin and that additional MSC were directly applied onto the surface of the open wound. We used human MSC, but that is not likely the cause of the difference as our recipients were immunodeficient NOD/SCID mice in which the reduction of the implanted cells over time<sup>40</sup> is similar to that noted by Wu<sup>36</sup>. Microscopically, the epidermal repair, which is slowed in irradiated skin, was not enhanced by the administration of MSC either.

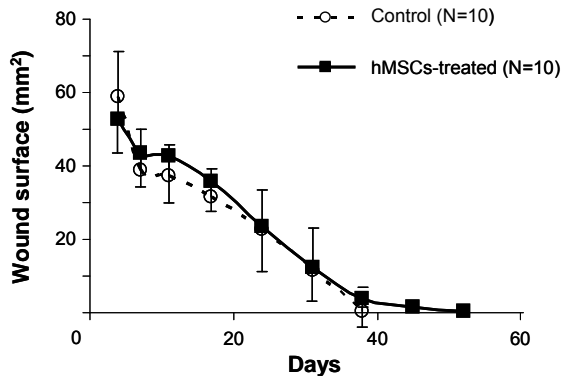


**Figure 4.8 Effect of MSC implants on ulcer healing.** Averages and SEM of ulcer surface of pre-irradiated decubitus without (control; open circles, upper vertical lines) and with MSC (MSC-treated; closed squares, lower vertical lines) injected are plotted. PU were induced by 12 hours of pressure.

Of considerable interest is the observation of different distribution of the injected cells in the ulcerated skin as compared to normal skin, a difference that held for both non-irradiated and pre-irradiated skin. There was less clustering and more spreading of the cells in the presence of decubitus, which may be attributed to a change in microenvironment in the surrounding tissue, e.g. inflammation.

Similar to observations in excisional skin wounds<sup>36</sup> is our finding of transdifferentiation of some MSC early after implantation and that these transdifferentiated cells have largely vanished at 30 days. Apparently, the early phase of repair favors MSC reprogramming and the subsequent tissue remodeling involves the loss of these differentiated cells either as a result of limited proliferation capacity or by active removal.

Small numbers of  $\beta$ -gal<sup>+</sup> myofibers were observed in the demarcation zone between the ulcer and the healthy tissue at all time points, in the control as well as in the pre-irradiated mice. The question arises if these blue fibers have originated from MSC that differentiated into the myogenic pathway or from fusion between MSC and mouse myofibers. The first mechanism cannot be entirely excluded, as an occasional blue cell with the morphology of myoblasts was seen in the demarcation zone of the PCM at 10 days after cell injection, not only in the control but also in the pre-irradiated PU. However, such differentiation cannot have proceeded through the normal pathway via satellite cells - that are characterized by high proliferation - because the number of  $\beta$ -gal<sup>+</sup> myofibers was not increased at 30 days.

In conclusion, our results show that the contribution of MSC to the repair of PU in our model is negligible which contrasts rather markedly with the published observations on excisional skin wounds.

The nature of the PU prevents direct application of MSC onto the lesion - as in excisional wounds - so that the significance of this factor remains uncertain. If the reported beneficial effects of MSC on wound healing are to be ascribed to paracrine factors, such a mechanism is clearly not effective in the case of PU.

The combined results of this study emphasize that PU respond differently to modifying influences than do surgical wounds. Finally, the PU model presented here seems to be well suited for translational research into new treatment modalities.



## References

1. Husain T: An experimental study of some pressure effects on tissues, with reference to the bed-sore problem. *J Path Bact* 1953;66:347-358.
2. Swaim SF, Bradley DM, Vaughn DM, Powers RD, Hoffman CE. The greyhound dog as a model for studying pressure ulcers. *Decubitus* 1993;6:32-40.
3. Salcido R, Fisher SB, Donofrio JC, Bieschke M, Knapp C, Liang R, LeGrand EK, Carney JM. An animal model and computer-controlled surface pressure delivery system for the production of pressure ulcers. *J Rehabil Res Dev* 1995;32:149-161.
4. Daniel RK, Priest DL, Wheatly DC. Etiological factors in pressure sores: an experimental model. *Arch Phys Med Rehabil* 1981;62:482-498.
5. Kokate JY, Leland KJ, Held AM, Hansen GL, Kveen GL, Johnson BA, Wilke MS, Sparrow EM, Iazzo PA. Temperature-modulated pressure ulcers: a porcine model. *Arch Phys Med Rehabil* 1995;76:666-673.
6. Kosiak M: Ethiology of decubitus ulcers. *Arch Phys Med Rehabil* 1961;42:19-29.
7. Pierce SM, Skalak TC, Rodeheaver GT: Ischemia-reperfusion injury in chronic pressure ulcer formation: a skin model in the rat. *Wound Repair Regen* 2000; 8:68-76.
8. Reid RR, Sull Ac, Mogford JE, Roy N, Mustoe TA. A novel murine model of cyclic cutaneous ischemia-reperfusion injury. *J Surg Res* 2004;116:172-80.
9. Stadler I, Zhang R, Oskoui P, Whittaker MS, Lanzafame RJ. Development of a simple, noninvasive, clinically relevant model of pressure ulcers in the mouse. *J Invest Surg* 2004;17:221-227.
10. Lanzafame RJ, Stadler I, Coleman J, Haerum B, Oskoui P, Whittaker M, Zhang RY. Temperature-controlled 830-nm low-level laser therapy of experimental pressure ulcers. *Photomed Laser Surg* 2004;22:483-488.
11. Lanzafame RJ, Stadler I, Kurtz AF, Connelly R, Peter TA Sr, Brandon P, Olson D. Reciprocity of exposure time and irradiance on energy density during photoirradiation on wound healing in a murine pressure ulcer model. *Lasers Surg Med* 2007;39:534-542.
12. Saito Y, Hasegawa M, Fujimoto M, Matsushita T, Horikawa M, Takenaka M, Ogawa F, Sugama J, Steeber DA, Sato S, Takehara K. The loss of MCP-1 attenuates cutaneous ischemia-reperfusion injury in a mouse model of pressure ulcer. *J Invest Dermatol* 2008;128:1838-1851.
13. Michaels J, Churgin SS, Blechman KM, Greives MR, Aarabi S, Galiano RD, Gurtner GC. *db/db* mice exhibit severe wound-healing impairments compared with other murine diabetic strains in a silicone-splinted excisional wound model. *Wound Repair Regen* 2007;15:665-670.
14. Keswani SG, Katz AB, Lim FY, Zoltick P, Radu A, Alaei D, Herlyn M, Crombleholme TM. Adenoviral mediated gene transfer of PDGF-B enhances wound healing in type I and type II diabetic wounds. *Wound Repair Regen* 2004;12:497-504.
15. Greenwald DP, Shumway S, Zachary LS, LaBarbera M, Albear P, Temaner M, Gottlieb LJ. Endogenous versus toxin-induced diabetes in rats: a mechanical comparison of two skin wound-healing models. *Plast Reconstr Surg* 1993;91:1087-1093.
16. Langer S, Born F, Breidenbach A, Schneider A, Uhl E, Messmer K. Effect of C-peptide on wound healing and microcirculation in diabetic mice. *Eur J Med Res* 2002;25:502-508.
17. Tibbs MK: Wound healing following radiation therapy: a review. *Radiother Oncol* 1997;42:99-106.
18. Gorodetsky R, McBride WH, Withers HR: Assay of radiation effects in mouse skin as expressed in wound healing. *Radiat Res* 1988;116:135-144.
19. Knaän-Shanzer S, van de Watering MJ, der Velde-van Dijke I, Goncalves MA, Valerio D, de Vries AA. Endowing human adenovirus serotype 5 vectors with fiber domains of species B greatly enhances gene transfer into human mesenchymal stem cells. *Stem Cells* 2005;23:1598-1607.
20. van Tuyn J, Knaän-Shanzer S, van de Watering MJ, de Graaf M, van der Laarse A, Schalij MJ, van der Wall EE, de Vries AA, Atsma DE. Activation of cardiac and smooth muscle-specific genes in primary human cells after forced expression of human myocardin. *Cardiovasc Res* 2005;67:245-255.
21. de la Garza-Rodea AS, van der Velde I, Boersma H, Goncalves MA, van Bekkum DW, de Vries AA, Knaän-Shanzer S. Long-term contribution of human bone marrow mesenchymal stromal cells to skeletal muscle regeneration in mice. *Cell Transplant* 2011a;20:217-231.

22. Gonçalves MA, Pau MG, de Vries AA, Valerio D. Generation of a high-capacity hybrid vector: packaging of recombinant adenoassociated virus replicative intermediates in adenovirus capsids overcomes the limited cloning capacity of adenoassociated virus vectors. *Virology* 2001;288:236-246.
23. Knaän-Shanzer S, van der Velde-van Dijke I, van de Watering MJ, de Leeuw PJ, Valerio D, van Bekkum DW, de Vries AA. Phenotypic and functional reversal within the early human hematopoietic compartment. *Stem Cells* 2008;26:3210-3217.
24. de la Garza-Rodea AS, Knaän-Shanzer S, den Hartigh JD, Verhaegen AP, van Bekkum DW. Anomer-stabilized streptozotocin solution for the induction of experimental diabetes in mice (*Mus musculus*). *J Am Assoc Lab Anim Sci* 2010;49:40-4.
25. Budach W, Hartford A, Gioioso D, Freeman J, Taghian A, Suit HD. Tumors arising in SCID mice share enhanced radiation sensitivity of SCID normal tissues. *Cancer Res* 1992;52:6292-6296.
26. National Pressure Ulcer Advisory Panel: Pressure ulcers prevalence, cost and risk assessment: consensus development conference statement. *Decubitus* 1989;2:24-28.
27. Tsuji S, Ichioka S, Sekiya N, Nakatsuka T. Analysis of ischemia-reperfusion injury in a microcirculatory model of pressure ulcers. *Wound Repair Regen* 2005;13:209-215.
28. Park CJ, Clark SG, Lichtensteiger CA, Jamison RD, Johnson AJ. Accelerated wound closure of pressure ulcers in aged mice by chitosan scaffolds with and without bFGF. *Acta Biomater* 2009;5:1926-1936.
29. O'Connell MP: Positioning impact on the surgical patient. *Nurs Clin North Am* 2006;41:173-192.
30. Romano Di Pepe S, Mangoni A, Zambruno G, Spinetti G, Melillo G, Napolitano M, Capogrossi MC. Adenovirus mediated VEGF<sub>165</sub> gene transfer enhances wound healing by promoting angiogenesis in CD1- diabetic mice. *Gene Ther* 2002; 9:1271-1277.
31. Trousdale RK, Jacobs S, Simhaee DA, Wu JK, Lustbader JW. Wound closure and metabolic parameter variability in a *db/db* mouse model for diabetic ulcers. *J Surg Res* 2009; 151:100-107.
32. Gulati AK: The effect of X-irradiation on skeletal muscle regeneration in the adult rat. *J Neurosci* 1987;78:111-120.
33. Wakeford S, Watt DH, Partridge TA: X-irradiation improves mdx mouse muscle as a model of myofiber loss in DMD. *Muscle Nerve* 1991;14:42-50.
34. Quinlan JG, Lyden, Cambier M, Johnson SR, Michaels SE, Denman DL. Radiation inhibition of mdx mouse muscle regeneration, dose and age factors. *Muscle Nerve* 1995;18:201-206.
35. Quinlan JG, Cambier D, Lyden S, Dalvi A, Upputuri RK, Gartside P, Michaels SE, Denman D. Regeneration-blocked mdx muscle: in vivo model for testing treatment. *Muscle Nerve* 1997;20:1016-1023.
36. Wu Y, Chen L, Scott PG, Tredget EE. Mesenchymal stem cells enhance wound healing through differentiation and angiogenesis. *Stem Cells* 2007;25:2648-2659.
37. Chen L, Tredget EE, Wu PY, Wu Y. Paracrine factors of mesenchymal stem cells recruit macrophages and endothelial lineage cells and enhance wound healing. *PLoS One* 2008;3.4: e1886.
38. Wu Y, Zhao RC, Tredget EE: Concise review: bone marrow-derived stem/progenitor cells in cutaneous repair and regeneration. *Stem Cells* 2010;5:905-915.
39. McFarlin K, Gao X, Liu YB, Dulchavsky DS, Kwon D, Arbab AS, Bansal M, Li Y, Chopp M, Dulchavsky SA, Gautam SC. Bone marrow-derived mesenchymal stromal cells accelerate wound healing in the rat. *Wound Repair Regen* 2008;14:471-478.
40. de la Garza-Rodea AS, Verweij MC, Boersma H, van der Velde-van Dijke I, de Vries AA, Hoeben RC, van Bekkum DW, Wiertz EJ, Knaän-Shanzer S. Exploitation of herpesvirus immune evasion strategies to modify the immunogenicity of human mesenchymal stem cell transplants. *PLoS One* 2011b;6:e14493.

